



PERGAMON

Solid State Communications 124 (2002) 63–66

solid  
state  
communications[www.elsevier.com/locate/ssc](http://www.elsevier.com/locate/ssc)

# Quasiparticle calculations of band offsets at AlN–GaN interfaces

Daniel Cociorva\*, Wilfried G. Aulbur, John W. Wilkins

*Department of Physics, Ohio State University, 174 W 18th Avenue, Columbus, OH 43210, USA*

Received 24 October 2001; received in revised form 3 June 2002; accepted 2 July 2002 by S.G. Louie

## Abstract

A first-principle quasiparticle theory in the GW approximation is used to compute valence and conduction band offsets, VBO and CBO, respectively, for hexagonal and cubic AlN–GaN interfaces. We find type I band offsets that depend on the in-plane lattice constant of the heterostructure, ranging from VBO = 1.3 eV and CBO = 1.5 eV for the in-plane lattice constant of a 6H–SiC (0001) substrate to VBO = 0.8 eV and CBO = 1.8 eV for the in-plane lattice constant of a GaN (0001) substrate. This sensitivity may explain the range of experimental results for systems whose in-plane lattice constants could not be directly measured. © 2002 Published by Elsevier Science Ltd.

PACS: 78.20.Bh; 78.66.Fd

Keywords: A. Heterojunctions; A. Semiconductors; D. Electronic band structure; D. Optical properties

Group III nitride (InN, GaN, AlN) heterostructures are promising candidates for the fabrication of UV/visible optoelectronics and high-frequency devices. [1–3] The quality and properties of such nitride heterojunction devices directly depend on the values of the conduction and valence band offsets, the subject of considerable experimental [4–6] and theoretical [7–10] activity. Experimentally, the electrical and optical properties of heterostructures prepared and deposited by different techniques are quite different, and the corresponding values reported for VBO range from 0.5 eV [4] to 1.4 eV [6]. Theoretically, the properties of the wurtzite structure interfaces are more challenging to calculate, since they are influenced both by strain-induced and spontaneous polarization [10].

This paper presents a detailed study of AlN–GaN interfaces, in both the zincblende and wurtzite structures. The many body effects, included in the calculation in the GW approximation (GWA) [11,12], account for a few eV correction over the corresponding LDA band edge energies. Fig. 1 shows our main results: the conduction and valence band offsets strongly depend on the in-plane lattice constant of the growth substrate. Fig. 1 also shows that the choice of

Ga pseudopotential is crucial for the accuracy of this study: including Ga's  $n = 3$  valence shell in the calculation is necessary to determine the offsets.

We determine the valence band offset VBO by dividing it in two terms: [13–15] (1) the difference between the valence band edge energies in the two bulk materials,  $\Delta E_{\text{VBM}}$ , each edge being referred to the average bulk electrostatic potential, and (2) the step  $\Delta V$  in the macroscopic average of the electrostatic potential across the interface

$$\text{VBO} = \Delta E_{\text{VBM}} + \Delta V. \quad (1)$$

The conduction band offset CBO is obtained by adding the computed band gap of each material.

## 1. Interface potential step

LDA accurately determines ground state properties; thus a self-consistent calculation of the electronic charge density at the interface yields the potential step  $\Delta V$ . We study four supercell orientations, wurtzite (0001) and zincblende (001), (110) and (111), at in-plane lattice constants simulating AlN, GaN and 6H–SiC substrates, and at the in-plane lattice constant equal to the average of AlN and GaN lattice constants. An interface orientation and in-plane lattice

\* Corresponding author. Tel.: +1-614-292-6386; fax: +1-614-688-3871.

E-mail address: [cociorva@pacific.mps.ohio-state.edu](mailto:cociorva@pacific.mps.ohio-state.edu) (D. Cociorva).

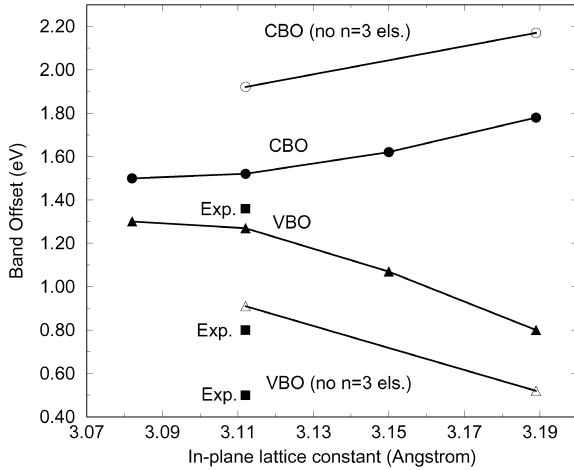


Fig. 1. Calculated (0001) AlN–GaN valence and conduction band offsets (solid triangles and circles, respectively), and experimental data (solid squares) from Ref. [4] (VBO = 0.5 eV), Ref. [5] (VBO = 0.8 eV), and Ref. [6] (VBO = 1.36 eV). Results of calculations using a simpler Ga pseudopotential, including only  $n = 4$  states, typically differ by 0.3–0.4 eV from those explicitly treating the  $n = 3$  states as well (valence band offset—empty triangles, conduction band offset—empty circles). The band offsets depend strongly on the in-plane lattice constant; a 3% variation of the substrate lattice constant changes the offsets by 0.5 eV. This may explain the range of the available experimental results, since it may be difficult to accurately monitor the in-plane lattice constant of the heterostructure interface. Since the effective in-plane lattice constants at the experimental interfaces could not be directly measured [4–6] in this figure we have assigned them, for simplicity, the AlN in-plane lattice constant.

constant define specific unit cell geometry. Within such a unit cell, the atomic positions are relaxed so that the atomic forces are less than 0.001 hartree/Bohr. The perpendicular (out-of-plane) lattice constant is determined by minimizing the total energy.

Fig. 2 shows the polar feature of the wurtzite AlN–GaN (0001) superlattice: the asymmetric interface charge distribution generates ‘uniform’ electric fields in the bulk of the two materials, away from the interface regions. In Fig. 2, the charge density at the AlN–GaN (0001) interface is decomposed into interface dipole and monopole; the interface dipole determines  $\Delta V$ , while the interface monopole determines the electric fields in the bulk-like regions [10].

Table 1 shows the sensitivity of the potential step  $\Delta V$  at the wurtzite (0001) interface to the in-plane lattice constant. The charge transfer at the interface depends strongly on the interface strain: a 3% change in lattice constant produces approximately a 0.3 eV variation of the potential step<sup>1</sup>.

<sup>1</sup> The potential step is, of course, not a well defined quantity, as it depends on the choice of atomic pseudopotentials. However, for a given choice, the variation of the potential step with the in-plane lattice constant results in a variation of the band offsets.

Table 1

Calculated band gaps, potential steps, and band offsets between GaN and AlN in wurtzite (0001) superlattices, along with measured valence band offsets. All energies are in eV. The dependence of the potential step on the lattice constant of the underlying substrate is primarily responsible for the variation in band offsets. Since the effective in-plane lattice constants at the experimental interfaces are not known, in this table we have assigned them, for simplicity, the AlN in-plane lattice constant

Wurtzite (0001)				
Substrate	6H–SiC	AlN	GaN	
Lattice const. $a_0$ (Å)	3.08	3.11	3.15	3.19
<i>GWA calculations</i>				
GaN band gap	3.30	3.29	3.22	3.13
AlN band gap	6.10	6.08	5.91	5.71
Potential step	0.93	0.91	0.76	0.60
VBO	1.30	1.27	1.07	0.80
CBO	1.50	1.52	1.62	1.78
<i>Experiments</i>				
VBO <sup>a</sup>	0.5 ± 0.2			
VBO <sup>b</sup>	0.8 ± 0.3			
VBO <sup>c</sup>	1.36 ± 0.07			

<sup>a</sup> From Ref. [4].

<sup>b</sup> From Ref. [5].

<sup>c</sup> From Ref. [6].

## 2. Bulk AlN and GaN band structures

Within the past decade, the GWA has been established [16] as the standard method for calculating quasiparticle band structures. Unlike LDA, GWA correctly describes excitation energies in semiconductors and insulators. The behavior of the quasiparticle wave function  $\Psi_{n\mathbf{k}}$  and energy  $E_{n\mathbf{k}}$  is governed by the quasiparticle equation

$$\left[ -\frac{1}{2}\nabla^2 + V_{\text{H}} + V_{\text{ext}} \right] \Psi_{n\mathbf{k}}(\mathbf{r}) + \int \Sigma(\mathbf{r}, \mathbf{r}'; E_{n\mathbf{k}}) \Psi_{n\mathbf{k}}(\mathbf{r}) = E_{n\mathbf{k}} \Psi_{n\mathbf{k}}(\mathbf{r}). \quad (2)$$

The central object of this equation is the quasiparticle self-energy  $\Sigma$ , a non-Hermitian, energy-dependent, non-local operator that describes exchange and correlation effects beyond the Hartree approximation. In GWA,  $\Sigma$  is expressed as the convolution of the dressed Green function  $G$  and the dynamically screened interaction  $W$

$$\Sigma(\mathbf{r}, \mathbf{r}'; E) = \frac{i}{2\pi} \int d\omega G(\mathbf{r}, \mathbf{r}'; E - \omega) W(\mathbf{r}, \mathbf{r}'; \omega). \quad (3)$$

In practice, the operator  $G$  is constructed from LDA wavefunctions, and  $W$  is evaluated by the random phase approximation [11,12] and a plasmon-pole model [17] to include the dynamics of screening. The difference between the self-energy operator and the LDA exchange-correlation potential  $V_{\text{xc}}$  constitutes a perturbation operator whose diagonal matrix elements are the quasiparticle corrections to

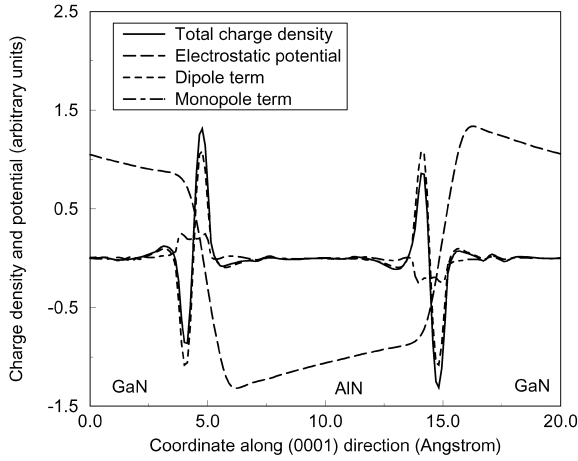


Fig. 2. Charge density and electrostatic potential in the (0001) AlN–GaN superlattice. The charge density is divided into its dipole and monopole components; [10] the dipole component produces the interface potential step, determining the conduction and valence band offsets. The monopole component determines the net electric field inside each bulk region.

the LDA band structure

$$E_{n\mathbf{k}} = E_{n\mathbf{k}}^{\text{LDA}} + \langle n, \mathbf{k} | \Sigma - V_{\text{xc}} | n, \mathbf{k} \rangle. \quad (4)$$

In AlN and GaN, the quasiparticle corrections are sizeable, shifting the positions of the valence band maxima with respect to the average electrostatic potential, and opening up the band gaps. As the quasiparticle shifts are not identical in the two materials, the band offsets change from their LDA values. The unstrained bulk AlN band gap is corrected from 4.12 eV in LDA to 6.08 eV in GWA, while the unstrained GaN band gap changes from 2.10 eV in LDA to 3.13 eV in GWA. Table 1 shows the calculated AlN and GaN band gaps for the four different in-plane lattice constants considered.

The choice of Ga pseudopotential affects the GaN bulk band gaps. Since Ga has localized d states, an accurate description of these states by GWA is possible only if Ga core 3s and 3p electrons are included in the calculation [18]. Including only the semicore Ga 3d states yields a *non-diagonal* perturbation matrix  $(\Sigma - V_{\text{xc}})_{mn}$ . Thus the determination of quasiparticle energies using Eq. (4) is not possible, as the LDA wavefunctions  $\Psi^{\text{LDA}}$  disagree with the quasiparticle wave functions  $\Psi^{\text{GWA}}$ . The same non-diagonality effect has been observed for CdS [18] and ZnS [19], which also have complete semicore d shells. Furthermore, the band gaps and the energies of the semicore d electrons deviate from experiment by as much as 3 eV. The consistent approximation to obtain the correct quasiparticle band structure is to use a Ga pseudopotential with the entire Ga  $n = 3$  electronic shell. Although the LDA results (charge density, lattice constant) are unchanged, the GWA perturbation matrix becomes diagonal in the new

basis set. The band gaps and the energies of the d states are now in good agreement with experiment.

### 3. Technical details

For LDA calculations we use Troullier–Martins pseudo-potentials [20,21] in the Kleinman–Bylander form [22–24], and the core states are taken into account by using non-linear core corrections. The LDA correlation potentials use the Perdew–Zunger parameterization [25] of the Ceperley–Alder quantum Monte Carlo data [26]. We choose energy cut-offs of 25 or 35 Hartrees, where the Ga  $n = 3$  electrons are treated as core and valence states, respectively. For AlN–GaN supercells we chose Monkhorst–Pack  $k$ -point meshes [27] with up to nine special  $k$ -points in the irreducible Brillouin zone. For most calculations, however, three or four special  $k$ -points prove to be sufficient for a very good convergence of the ground state charge density. In these cases, the LDA eigenvalues are within 10 meV of those produced by denser nine special  $k$ -point meshes.

The GWA calculations for bulk AlN and GaN are carried out at the relaxed LDA lattice constants. We use the equivalent of 10 special  $k$ -points in the irreducible Brillouin zone to determine the ground state density, the dielectric matrix, and the self-energy corrections. We keep 200 conduction bands in the determination of the dielectric matrix, and a reciprocal space cut-off of 5.0 a.u. The energy dependence of the dielectric matrix is approximated by the Engel–Farid plasmon pole model [17]. The number of plasmon pole bands summed for the determination of the self-energy is 150. All these parameters have been checked for convergence, and produce an overall convergence error of less than 50 meV [28]. Self-energy corrections are determined in first-order perturbation theory, without updating the energies in the Green function. This standard approach works well in practical applications, and generally leads to good agreement with experiment for quasiparticle energies [16].

### 4. Results

Tables 1 and 2, and Fig. 1 summarize our results. In Fig. 1, the valence band offset decrease with the lattice constant is mainly due to the decrease in the potential step in Table 1, arising from the strain-induced variation of the electronic charge density. The conduction band offset increase with the lattice constant is also mostly due to the same potential step variation. Any additional change in the conduction band offset is due to the larger decrease of AlN band gap, compared to GaN band gap, with respect to the in-plane lattice constant. The dependence of the offsets on the lattice constant of the substrate may explain the large experimental discrepancies. For example, the valence band offset varies

Table 2

Calculated valence and conduction band offsets between GaN and AlN in zincblende (001), (110) and (111) superlattices as a function of in-plane lattice constant  $a_0$ . All energies are in eV. No experimental data is available for comparison. Note the weak dependence of the offsets on the interface orientation

Substrate	AlN		GaN
Lattice const. $a_0$ (Å)	4.38	4.44	4.50
<i>Zincblende</i> (001)			
VBO	1.02	0.92	0.76
CBO	0.68	0.70	0.78
<i>Zincblende</i> (110)			
VBO	1.06	0.95	0.81
CBO	0.64	0.67	0.73
<i>Zincblende</i> (111)			
VBO	1.08	0.95	0.80
CBO	0.62	0.67	0.74

from 0.8 eV for a GaN substrate to 1.3 eV for a 6H–SiC (0001) substrate. This is roughly the same range of values as that of experimental results. Possibly the range of experimental results can be attributed to different growth conditions [4] and, hence, different in plane lattice constants.

Many-body effects are significant: our LDA valence band offsets are typically 0.2–0.4 eV lower than those obtained by GWA, in Tables 1 and 2. They are in good agreement with LDA numbers reported by other groups [7–10]. Also, since GWA allows the determination of AlN and GaN band gaps, we can additionally report first principles conduction band offsets. Table 2 shows that, for the zincblende crystal structure, the band offsets depend very weakly on the interface orientation. The difference in band offsets between zincblende (001), (110), and (111) interfaces is less than 0.1 eV. Furthermore, the crystal field splitting of the valence band top is rather small, of the order of 10 meV.

## 5. Conclusion

This paper presents a GWA calculation of band offsets in AlN–GaN, including important effects of interface strain, polarization fields, and Ga core states. We report significant trends, such as the dependence of the valence and conduction band offsets on the in-plane lattice constant, as well as on the choice of Ga pseudopotential used. We confirm that large macroscopic polarization fields exist in the bulk regions of the polar (0001) superlattice, and a charge density decomposition in monopole and dipole terms is necessary in order to determine the electrostatic potential step  $\Delta V$ . We find that the variation of  $\Delta V$  with the in-plane lattice constant is the determining factor in the variation of

the band offsets and we explain the discrepancies between the available experimental results by differences in the in-plane lattice constants of those AlN–GaN heterostructures.

## Acknowledgments

This work was supported by the NSF (contract DMR-0076362), the DOE-Basic Energy Sciences, Division of Materials Sciences (contract DE-FG02-99ER45795), and the SRC (contract 2000-MJ-759). Computer resources were provided by the Ohio Supercomputer Center.

## References

- [1] R.F. Davis, Proc. IEEE 79 (1991) 702.
- [2] J.H. Edgar, J. Mater. Res. 7 (1992) 235.
- [3] S.N. Mohammed, A.A. Salvador, H. Morkoc, Proc. IEEE 83 (1995) 1306.
- [4] S.W. King, C. Ronning, R.F. Davis, M.C. Benjamin, R.J. Nemanich, J. Appl. Phys. 84 (1998) 2086.
- [5] G. Martin, A. Botchkarev, A. Rockett, H. Morkoc, Appl. Phys. Lett. 68 (1996) 2541.
- [6] J.W. Waldrop, R.W. Grant, Appl. Phys. Lett. 68 (1996) 2879.
- [7] E. Albanesi, W.R. Lambrecht, B. Segall, J. Vac. Sci. Technol. B 12 (1994) 2470.
- [8] S. Wei, A. Zunger, Appl. Phys. Lett. 65 (1996) 610.
- [9] M.B. Nardelli, K. Rapcewicz, J. Bernholc, Phys. Rev. B 55 (1997) R7323.
- [10] F. Bernardini, V. Fiorentini, Phys. Rev. B 57 (1998) R9427.
- [11] L. Hedin, Phys. Rev. 139 (1965) A796.
- [12] L. Hedin, S. Lundqvist, in: F. Seitz, D. Turnbull, H. Ehrenreich (Eds.), Solid State Physics, vol. 23, Academic Press, New York, 1969, p. 1.
- [13] A. Baldereschi, S. Baroni, R. Resta, Phys. Rev. Lett. 61 (1988) 734.
- [14] S.B. Zhang, D. Tomanek, S.G. Louie, M.L. Cohen, M.S. Hybertsen, Solid State Commun. 66 (1988) 585.
- [15] S.B. Zhang, M.L. Cohen, S.G. Louie, D. Tomanek, M.S. Hybertsen, Phys. Rev. B 41 (1990) 10058.
- [16] W.G. Aulbur, L.W. Jönsson, J.W. Wilkins, Solid State Phys. 54 (1999) 1 and references therein.
- [17] G.E. Engel, B. Farid, Phys. Rev. B 47 (1993) 15931.
- [18] M. Rohlfing, P. Krüger, J. Pollmann, Phys. Rev. Lett. 75 (1995) 3489.
- [19] O. Zakharov, A. Rubio, X. Blase, M.L. Cohen, S.G. Louie, Phys. Rev. B 50 (1994) 10780.
- [20] N. Troullier, J.L. Martins, Phys. Rev. B 43 (1991) 8861.
- [21] N. Troullier, J.L. Martins, Solid State Commun. 74 (1990) 613.
- [22] D.M. Bylander, L. Kleinman, Phys. Rev. B 55 (1997) 9432.
- [23] D.M. Bylander, L. Kleinman, Phys. Rev. B 54 (1996) 7891.
- [24] D.M. Bylander, L. Kleinman, Phys. Rev. B 52 (1995) 14566.
- [25] J.P. Perdew, A. Zunger, Phys. Rev. B 23 (1981) 5048.
- [26] D.M. Ceperley, B.I. Alder, Phys. Rev. Lett. 45 (1980) 566.
- [27] H.J. Monkhorst, J.D. Pack, Phys. Rev. B 13 (1976) 5188.
- [28] W.G. Aulbur, PhD Thesis, The Ohio State University, 1996.